Contents lists available at SciVerse ScienceDirect

Surface Science

Hard X-ray photoemission spectroscopy: Variable depth analysis of bulk, surface and interface electronic properties

Giancarlo Panaccione [a,*], Keisuke Kobayashi [b,c]

[a] Istituto Officina dei Materiali (IOM)-CNR, Laboratorio TASC, in Area Science Park, S.S.14, Km 163.5, I-34149 Trieste, Italy
[b] Hiroshima Synchrotron radiationCenter, Hiroshima University, 2–313 Kagamiyama, Higashi-Hiroshima, Japan
[c] NIMS beamline Station at Spring-8, National Institute for Materials Science, Sayo, Hyogo 679–5148, Japan

ARTICLE INFO

ABSTRACT

The electronic properties of surfaces and buried interfaces can vary considerably in comparison to the bulk. In turn, analyzing bulk properties, without including those of the surface, is understandably challenging. Hard X-ray photoelectron spectroscopy (HAXPES) allows the well known ability of photoemission to interrogate the electronic structure of material systems with bulk volume sensitivity. This is achieved by tuning the kinetic energy range of the analyzed photoelectrons in the multi-keV regime. This unique ability to probe truly bulk properties strongly compliments normal photoemission, which generally probes surface electronic structure that is different than the bulk selected examples of HAXPES and possible implications towards the study of complex oxide-based interfaces and highly correlated systems are discussed.

Almost every possible physical property changes at the surface of a solid system: the modifications induced by both the broken symmetry and the reduced dimensionality on the electronic and crystalline structure have a profound influence on the macroscopic behavior of the solid as a whole. This is observed in terms of optical properties, hyperfine fields, magnetism, thermal and electric conduction to name but a few. The surface also represents a peculiar interface system, the extreme limit between the solid and the vacuum, and, as such, an incredible variety of anomalous properties and new physical phenomena have been found at the interface also, in their natural or artificial form [1,2]. The prospective of a quasi-limitless access to new science based on surface and interface effects has led to a tremendous theoretical and experimental effort, evolving, in the last four decades, from 'classic' surface science to the advent of 'nanoscience' [3,4]. It is clear that detailed knowledge on the surface/interface vs. bulk electronic properties is critical, coupled with a deep understanding of the mechanisms involved, if these systems are to find any technological application.

A clear example of this difficulty can be found in the study of strongly correlated systems such as low dimensional artificial solids and complex oxides, where a broad range of behaviors from insulating to metallic, magnetic and even superconducting behavior depend upon minute changes – the energy scale of the relevant processes lies in the meV regime – of the electron, spin, and orbital degrees of freedom [5]. Analysis of such an important aspect requires on one hand the ability to probe structural, electronic and magnetic properties with chemical sensitivity, while on the other, a full control of the depth information acquired (i.e. surface to near-surface to bulk).

Looking at the spectroscopic tools available, only a few analytical methods qualify: photoemission spectroscopy (PES), and in particular X-ray based PES, is one of the most powerful techniques to investigate the electronic structure of solid state materials. PES is a versatile technique, easy to use and relatively non-destructive, with the combination of PES and Synchrotron Radiation (SR), over the last 30 years, has proven extremely fruitful in surface and interface studies. A strong surface sensitivity, of the order of 5 Å, i.e. a few atomic layers, can be achieved by tuning the energy of the incoming SR to the minimum of the escape depth of the outgoing photoelectrons, as depicted in Fig. 1 [6,7]. Today, PES experiments with state-of-the-art energy and momentum resolution provide the most detailed information on the electronic states at the surface of solids. On the other hand, there is an almost complete lack of corresponding experimental PES information on truly bulk properties.

The most direct way for increasing the probing depth in PES experiments is to increase or decrease the excitation energy, and correspondingly the kinetic energy of the outgoing photoelectron [8]. Although more straightforward from a technical point of view, extremely low energy PES has some crucial drawbacks, due to the limited kinetic energy range available (core level PES is impossible), along with the influence of final state effects and a material dependency on probing depth. Hard X-ray photoemission spectroscopy (HAXPES) experiments were originally pioneered by Pianetta and Lindau in 1974 [9], and have recently been revived by several research groups since 2003 [10–19]. With the advent of 3rd generation synchrotrons, the ability to exploit HAXPES, with the necessary high flux ($10^{11}/10^{12}$ photons/s on the sample in a bandwidth of 50–300 meV) to overcome the strong reduction of

* Corresponding author.
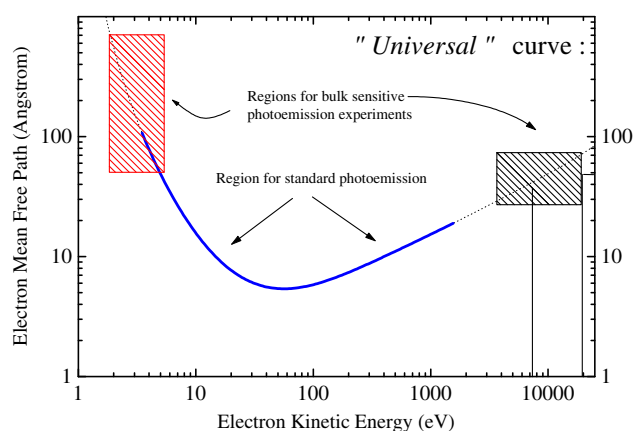 E-mail address: giancarlo.panaccione@elettra.trieste.it (G. Panaccione).

Fig. 1. The universal curve of the escape depth of photoelectrons [6,7]. The shaded boxes indicate the regions where bulk sensitive photoemission is possible. The high kinetic energy region concerns HAXPES experiments.

photo-ionization cross section at high energy [20], as well as the extremely large dynamic range in photon energy (4 to 15 keV). A very respectable limited energy resolution (~ 50 meV), is more than good enough to obtain reliable comparison with standard surfaces sensitive PES. HAXPES measurements provide information from a depth of up to 15–20 nm for electron kinetic energies > 5 keV, corresponding to truly bulk sensitivity with chemical selectivity [21]. The scope of this paper is to present selected examples, which describe recent important results, as well as future developments of the HAXPES technique.

An example that epitomizes the capabilities of HAXPES comes in the determination of the Fermi level and/or of the surface carrier accumulation of complex oxides. Many of these systems can neither be prepared with standard surface science techniques, nor display the same (electronic) properties between surface and bulk, hence genuine bulk sensitivity is required. Moreover, the strong variation of cross section when passing from soft to Hard X-ray can be used to advantage, for example, to highlight the metal *s* contribution of the total density of states in valence band photoemission in materials of the post-transition metals. In fact, although the cross section of all states is severely suppressed in the HAXPES regime (up to a factor 10^{-4}), the relative ratio of states with different symmetry strongly favors extended *s*-states with respect to localized *p*, *d* and *f* ones. Consider the case of PbO_2, a widely used *metallic* conductor of electricity in lead acid batteries. Although almost all binary oxides where the metal atom achieves the group oxidation state are insulators (e.g., TiO_2, ZrO_2, HfO_2, ThO_2, GeO_2 and SnO_2, all of which have gaps in excess of 3 eV [22,23]), β-PbO_2 is a metallic conductor [24] where the metallic nature of PbO_2 has been the subject of conjecture. On the basis of bandstructure calculations it has been suggested that PbO_2 is intrinsically metallic due to overlap of the top of the valence band of O 2p states with the bottom of the conduction band comprised of Pb 6s states. On the other hand the conduction electron concentration is known to vary with preparation conditions in a way suggestive of population of conduction band states by carriers introduced by oxygen vacancy defects or proton interstitials [25]. A clear path towards resolution of this controversy lies in the measurement of photoemission spectra which locate the position of the metallic Fermi edge relative to the edge of the O 2p dominated valence band. To date however it has proved problematic to observe conduction band states in conventional photoemission experiments due to the low carrier concentration and the dominance of O 2p states in the measured spectra — for example at 56.0 eV photon energy the conduction band structure is two to three orders of magnitude weaker than the valence band structure (Fig. 2). Payne et al. approached the problem of PbO_2 with the use of HAXPES [26,27]. At a photon energy of ~8 keV, the photo-ionization cross sections of Pb 6s states is almost two orders of magnitude larger

than the cross sections for ionization of O 2p states. As seen in Fig. 2, the intensities of bands II and III increase relative to that of band I as the incident photon energy increases and at 7700 eV photon energy band III is the dominant component of the valence band . Bandstructure calculations show that band I relates to states of almost pure O 2p character, mixing between O 2p states and Pb 6p orbitals if found in states contributing to band II, and band III band III involve an equal mix of Pb 6s and O 2p character [26,27]. The variation of states I, II, and III as a function of photon energy, allowed clarification that the Pb 6s contribution is higher (relative to the O 2p contribution) at the bottom of the valence band than in the conduction band. This experimental evidence is at variance with a purely ionic model, which presupposes that no Pb 6s character should be present in the valence band. HAXPES valence band spectra show a well-defined metallic Fermi edge of PbO_2 sitting well above the main valence band edge, with clear evidence of an incipient gap between the valence and conduction bands (Fig. 2). These experiments thus provide clear evidence in favor of the "defect" hypothesis. The population of this band most likely arises from donor states associated with oxygen vacancies.

Looking at the broader implications of the presented results, cross sections for ionization of 4s and 5s orbitals are similar to those for 6s orbitals at high energies [28,29]. It follows that selective enhancement of the metal *n*s contribution to the cross section weighted density of states is expected to be a general feature of high energy photoemission. This has also been of particular value in the study of conduction band states in n-type transparent conducting oxides such undoped and Sn-doped In_2O_3, where, with the help of the bulk sensitive probe HAXPES, it has been shown that: a) the bandgap is direct with an upper limit on the fundamental band gap of 2.9 eV [30], well below the widely quoted band gap of 3.75 eV and b) the comparison between the valence band edge spectra measured at $h\nu = 1486.6$ eV and $h\nu = 6000.0$ eV reveals a pronounced accumulation of electrons close to the surface. At the same time HAXPES enables identification of the regions of O 2p valence bands that are hybridized with cation *s* states for any oxide, thus being able to quantify the ionic/metallic character of complex oxides. In addition, several HAXPES studies have been devoted to the study of band gap states and conduction band filling due to extrinsic carriers in thin films of ZnO [31,32,33], InGaZnO [34,35], and InN [36]. Also due to the large probing depth, HAXPES may also probe buried interfaces under 'in operando' situations, e.g. while applying electric field through the surface electrode. Examples of this type of application are the detection of mid-gap interface states in a C-MOS structure [37] and the monitoring of the metal–oxide interface during electrochemical reactions in resistance memory devices [38,39]. Development of the 'in operando' approach should address present technological and experimental aspects, as e.g. i) a top electrode thickness in the range 10 to 20 nm, to guarantee a sizeable intensity from the buried region signal intensity from the region beneath, ii) a careful selection of materials for electrodes, to obtain continuous and smooth layers. Moreover, it should be noted that a small electron diffusion length in the resistive top electrode layer may cause inhomogeneous electric field distribution in the target layer when current (due to tunneling or other leakage) flows between the top and the bottom electrode. Large 2D carrier concentrations at interfaces cause metallic screening, which may strongly modify the potential profiles. This effect may represent a serious obstacle if the screening length becomes shorter than the electron attenuation length of ca. 10 nm.

Although HAXPES originates at large scale facilities, recent developments concern the use of laboratory-based HAXPES, with clear advantages in terms of experimental control, sample environment and flexibility of operation. In a laboratory-based HAXPES setup with practical throughput one needs to overcome the debilitating decrease of signal intensity due to the rapid reduction in photo-ionization cross sections accompanied with increasing photon energy. Consequently the crucial aspects are to design a monochromatic X-ray source with
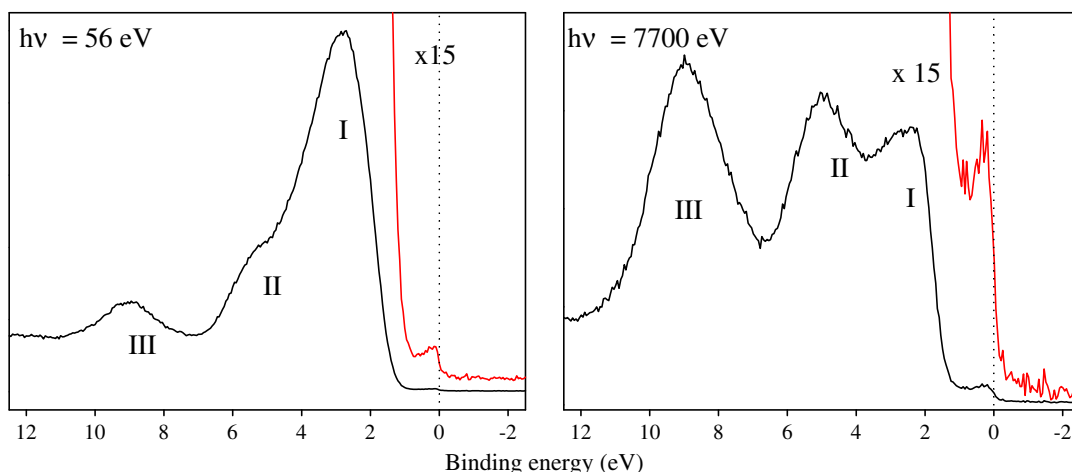
Fig. 2. Photoemission spectra of β-PbO₂ excited at 56 eV and 7700 eV photon energy. Note the dramatic increase in the relative intensity of the conduction band photoemission feature (highlighted in red). The highest valence band state III also increases in relative intensity. Both states I and III have substantial Pb 6s character.

high-flux and an electron analyzer with wide acceptance. Recently a High Energy Angle Resolved Photoelectron Spectrometer for Laboratory uses (HEARP Lab) with adequate performances has been achieved [40]. The system consists of a focused Cr Kα source, a wide acceptance objective lens, and a high energy version of VG Scienta R4000 analyzer. The X-ray source is designed in a similar way to the VersaProbe (ULVAC-PHI, Inc.) Al Kα source. The Cr Kα (5.4 Kα KeV) X-rays emitted from a water cooled Cr target bombarded by a focused electron beam are monochromatized and focused onto a sample surface by a compact bent crystal monochromator with a 300 mm Roland circle. The X-ray spot size is variable from 10 μm (1.25 W) to 200 μm (50 W). The wide-acceptance objective lens designed by Matsuda and Daimon using an ellipsoidal mesh electrode in the first stage of the lens is installed in front of the hemispherical analyzer [41]. Basic performances of the whole laboratory system were evaluated by measuring 3d core level and valence band spectra of Au [40], resulting in a total energy resolution of 0.53 eV. Angular acceptance and angular resolution were evaluated as ±35° and a less than 0.5°, respectively. An additional

feature of the HEARP Lab was the observation of bulk X-ray photoelectron diffraction (XPD). Hard X-ray regime XPD is expected as one of the useful techniques to open up possibilities in accessing bulk local atomic structures of a wide variety of materials. The HXPD measurements were performed on the Si 1s core level photoelectrons, at kinetic energy 3569 eV, from a Si(001) substrate covered by a hydrogen terminated, 4 nm-thick and 7 nm-thick silicon dioxide overlayers were measured with an angular resolution of 0.5° in the polar direction and with 3° step in the azimuthal direction [42]. The experimental configuration is schematically shown in Fig. 3(a). The azimuthal angle was scanned in the range of over 90°. A rotational symmetry operation was applied, considering the symmetry of the crystal. The measurement time required for one pattern was approximately 30 h. Theoretical studies predicted that the electron-atom scattering process at high kinetic energies produce a strong enhancement of the intensity in the forward scattering, which should provide real-space information on the directions of near-neighbor bonds and low-index axes. Fig. 3(b) shows a experimental HXPD pattern of hydrogen terminated Si(001) substrate. The positions
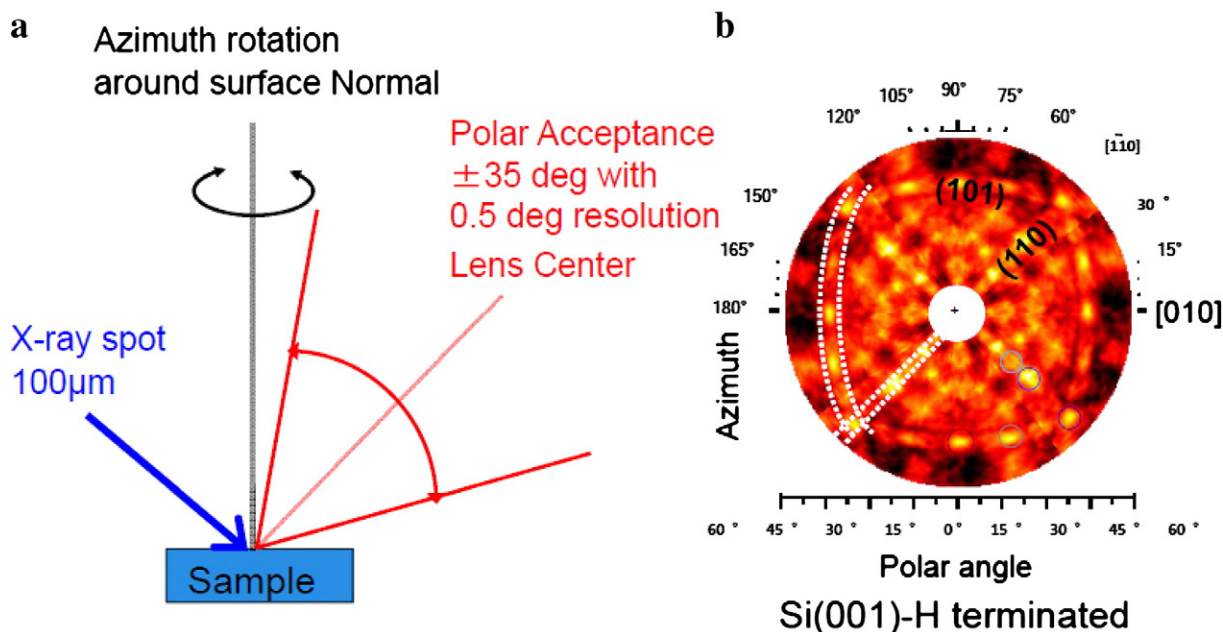

Fig. 3. (a) Schematic drawing of experimental configuration for HXPD measurements using HEARP Lab. (b) HXPD 2D pattern of hydrogen terminated Si(001). Some of the forward scattering spots and Kikuchi bands are denoted by small circles and dotted lines, respectively.

of the main spots are in good agreement with low-index directions in the silicon crystal structure. Other significant features in the HXPD pattern were lines of enhanced intensity along the [110] and [−110] directions. Their origin comes from a forward-focusing effect in the (110) plane and from long-order Bragg diffraction, which creates the well-known Kikuchi bands from (110) atomic planes. All these features were well reproduced by a cluster calculation. The forward scattering spots were clearly observed in samples with 4 nm thick oxide overlayers and distinguishable even in the 7 nm overlayer case, verifying the high bulk sensitivity of the HXPD.

A further application of HEARP Lab has been the thickness determination of nearly atomically flat SiO_2 overlayers, in order to verify the feasibility of the HEARP Lab in angular resolution mode [43]. Samples were prepared by the standard industrial thermal furnace oxidation process with the thickness of 4–25 nm on Si(001). The take off angle (TOA) dependences (measured from the normal emission angle of sample) of Si 1s spectra, found at1844.8 eV (oxide) and 1839.6 eV (substrate) binding energies, were measured in the TOA range of 30–90° with sample normal fixed at 30° from the analyzer axis (as Fig. 3(a)). The intensity of the oxide spectra smoothly varied with the TOA while those of the substrate exhibited strong modulations, due to the XPD effects discussed above. Continuous rotation of the sample around the axis normal to the sample surface during the measurements was effective in reducing the intensity modulation. The TOA dependences of the intensity ratio between the Si 1s peaks of the oxide (I_o) and the substrate (I_s) were analyzed by adopting a simple uniform overlayer-substrate model, which resulted in an excellent linear correlation with thickness values obtained by ellipsometry, with a gradient of 1.05 and a y-axis intercept of −0.3 in the overlayer thickness region of 4 nm–25 nm.

A further application, potentially relevant for new materials in semiconductors research, is presented in Fig. 4, where profiling of a gate stack model structure sample of Ir (8 nm)/HfO_2 (2.2 nm)/wedge shape SiO_2(0–10 nm)/Si(100) was performed by varying the X-ray spot position on the sample surface, with the same experimental setup of Fig. 3(a) [43]. With the goal of increasing the capacitance without increasing leakage current in CMOS gates, SiO_2 gate insulators thickness is set to 1 nm or less. Such small thicknesses of SiO2 give rise to radical increase of leak current, thus performances of high dielectric constant materials such as HfO_2 and related oxides are now explored. Trapped charge in these materials may cause additional scattering of the carriers, and reduced channel mobility. HAXPES analysis may help to evaluate the influence of trapped charges, via the analysis of core level shift.

The thickness profiling of a buried wedge shape SiO_2 layer in the same sample evidenced that the SiO_2 wedged layer was fabricated exactly as designed varying linearly from 0 to 10 nm with changing position from 0 to 2.5 mm. The intensity ratio of O 1s components which are to be identified as SiO_2 at 4876 eV and HfO_2 at 4878 eV varies with SiO_2 thickness. Si 1s (both substrate and oxides) peak shapes also depend on the SiO_2 thickness as shown in Fig. 3(b). No distinguishable variation with SiO_2 thickness in Hf $3d_{5/2}$ and Ir $3d_{5/2}$ was recognized. The shifts of the substrate and oxide Si 1s peaks are also plotted as functions of determined SiO_2 thickness in Fig. 3(c). This results suggest that these peak shifts are mainly due to charge trapped at the HfO_2–SiO_2 interface and the amount of charge is constant at least until the SiO_2 thickness does not exceed 7 nm. The result is consistent with the observation that channel mobility increases as thickness of SiO_2interlayer increases, due to reduction of Coulomb scattering of channel carriers by the trapped charges.

To conclude, Hard X-ray PES (HAXPES) may open new opportunities in the study of complex systems and interfaces, by exploiting the variable depth information of the high energy photoemission technique. In the mid-term future the optimized control of external
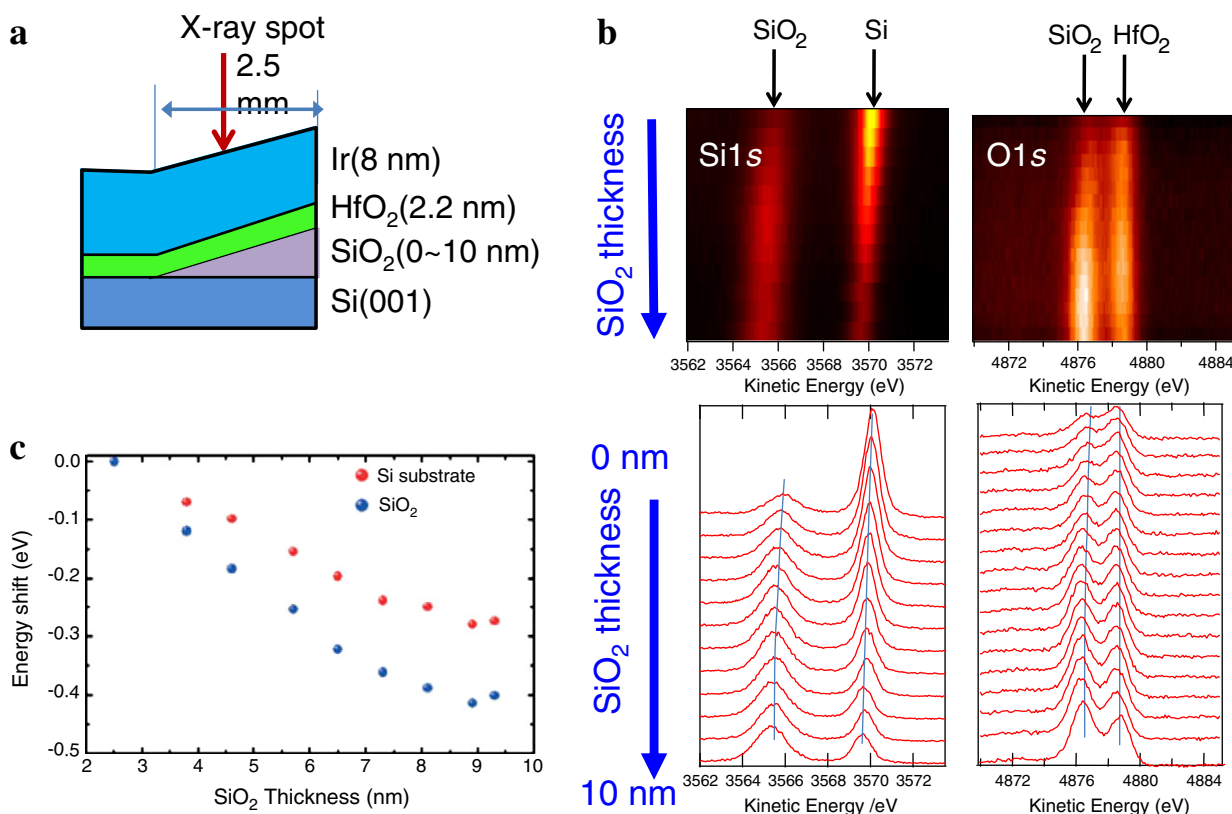

Fig. 4. (a) Schematic sample structure, (b) Si 1s and O 1s spectra measured in 200 µm steps along the thickness varying direction, (c)) dependent of Si 1s peaks on the SiO_2 thickness calculated from the intensity ratio I_o/I_s, where I_o and I_s are Si 1s intensities of the oxide and the substrate, respectively. (The resultant SiO_2 thickness was found to be linearly varying with the position change.).

parameters such as, electric field, temperature and pressure is foreseen, bringing HAXPES activity towards, the so far unexplored, 'in operando' regime, both at large-scale synchrotron facilities and in laboratory-based environments.

Acknowledgements

References

[1] A. Zangwill, Physics at Surfaces, Cambridge Univ. Press, 1988.
[2] H. Luth, Solid Surfaces, Interfaces and Thin Films, Springer, Berlin, 2001.
[3] J.V. Barth, G. Costantini, K. Kern, Nature 437 (2005) 671.
[4] C. Chappert, A. Fert, F. Nguyen Van Dau, Nature Mater. 6 (2007) 813.
[5] J. Goniakowski, F. Finocchi, C. Noguera, Rep. Prog. Phys. 71 (2008) 016501.
[6] S. Tanuma, C.J. Powell, D.R. Penn, Surf. Interface Anal. 43 (2011) 689;
    S. Tougaard, QUASES-IMFP-TPP2M Version 2.2, http://www.quases.com/2002.
[7] M.P. Seah, W. Dench, Surf. Interface Anal. 1 (1979) 2.
[8] A. Sekiyama, T. Iwasaki, K. Matsuda, Y. Saitoh, Y. Onuki, S. Suga, Nature 403 (2000) 396.
[9] I. Lindau, P. Pianetta, S. Doniach, F. Spicer, Nature 250 (1974) 214.
[10] K. Kobayashi, M. Yabashi, Y. Takata, T. Tokushima, S. Shin, K. Tamasaku, D. Miwa, T. Ishikawa, H. Nohira, T. Hattori, Y. Sugita, O. Nakatsuka, A. Sakai, S. Zaima, Appl. Phys. Lett. 83 (2003) 1005.
[11] C. Dallera, L. Duò, L. Braicovich, G. Panaccione, G. Paolicelli, B. Cowie, J. Zegenhagen, Appl. Phys. Lett. 85 (2004) 4532.
[12] P. Torelli, M. Sacchi, G. Cautero, M. Cautero, B. Krastanov, P. Lacovig, P. Pittana, R. Sergo, R. Tommasini, A. Fondacaro, F. Offi, G. Paolicelli, G. Stefani, M. Grioni, R. Verbeni, G. Monaco, G. Panaccione, Rev. Sci. Instrum. 76 (2005) 023909.
[13] G. Panaccione, M. Cautero, G. Cautero, A. Fondacaro, M. Grioni, P. Lacovig, G. Monaco, F. Offi, G. Paolicelli, M. Sacchi, M. Stojic, G. Stefani, R. Tommasini, P. Torelli, J. Phys. Condens. Matter 17 (2005) 2671.
[14] M. Taguchi, A. Chainani, K. Horiba, Y. Takata, M. Yabashi, K. Tamasaku, Y. Nishino, D. Miwa, T. Ishikawa, T. Takeuchi, K. Yamamoto, M. Matsunami, S. Shin, T. Yokoya, E. Ikenaga, K. Kobayashi, T. Mochiku, K. Hirata, J. Hori, K. Ishii, F. Nakamura, T. Suzuki, Phys. Rev. Lett. 95 (2005) 177002.
[15] M. Taguchi, A. Chainani, N. Kamakura, K. Horiba, Y. Takata, M. Yabashi, K. Tamasaku, Y. Nishino, D. Miwa, T. Ishikawa, S. Shin, E. Ikenaga, T. Yokoya, K. Kobayashi, T. Mochiku, K. Hirata, K. Motoya, Phys. Rev. B 71 (2005) 155102.
[16] K. Horiba, M. Taguchi, A. Chainani, Y. Takata, E. Ikenaga, D. Miwa, Y. Nishino, K. Tamasaku, M. Awaji, A. Takeuchi, M. Yabashi, H. Namatame, M. Taniguchi, H. Kumigashira, M. Oshima, M. Lippmaa, M. Kawasaki, H. Koinuma, K. Kobayashi, T. Ishikawa, S. Shin, Phys. Rev. Lett. 93 (2004) 236401.
[17] G. Panaccione, M. Altarelli, A. Fondacaro, A. Georges, S. Huotari, P. Lacovig, A. Lichtenstein, P. Metcalf, G. Monaco, F. Offi, L. Paolasini, A. Poteryaev, M. Sacchi, O. Tjernberg, Phys. Rev. Lett. 97 (2006) 116401.
[18] S. Suga, A. Sekiyama, S. Imada, A. Shigemoto, A. Yamasaki, M. Tsunekawa, C. Dallera, L. Braicovich, T.L. Lee, O. Sakai, T. Ebihara, Y. Onuki, J. Phys. Soc. Jpn. 74 (2005) 2880.
[19] Yamasaki, S. Imada, H. Higashimichi, H. Fujiwara, T. Saita, T. Miyamachi, A. Sekiyama, H. Sugawara, D. Kikuchi, H. Sato, A. Higashiya, M. Yabashi, K. Tamasaku, D. Miwa, T. Ishikawa, S. Suga, Phys. Rev. Lett. 98 (2007) 156402.
[20] J.J. Yeh, I. Lindau, At. Data Nucl. Data Tables 32 (1985) 1.
[21] M. Sacchi, F. Offi, P. Torelli, A. Fondacaro, C. Spezzani, M. Cautero, G. Cautero, S. Huotari, M. Grioni, R. Delaunay, M. Fabrizioli, G. Vankó, G. Monaco, G. Paolicelli, G. Stefani, G. Panaccione, Phys. Rev. B 71 (2005) 155117.
[22] R.D. Shannon, R.X. Fischer, Phys. Rev. B 73 (2006) 235111.
[23] Semiconductors: Physics of Non-Tetrahedrally Bonded Binary Compounds II, in: O. Madelung, Landolt-Börnstein (Eds.), New Series, Group III, Vol. 17, Springer Verlag, Berlin, 1984, Pt. f.
[24] P.T. Moseley, J.L. Hutchison, M.A.M. Bourke, J. Electrochem. Soc. 129 (1982) 876.
[25] J.P. Pohl, G.L. Schlechtriemen, J. Appl. Electrochem. 14 (1984) 521.
[26] D.J. Payne, R.G. Egdell, G. Paolicelli, F. Offi, G. Panaccione, P. Lacovig, G. Monaco, G. Vanko, A. Walsh, G.W. Watson, J. Guo, G. Beamson, P.-A. Glans, T. Learmonth, K.E. Smith, Phys. Rev. B 75 (2007) 153102.
[27] D.J. Payne, G. Paolicelli, F. Offi, G. Panaccione, P. Lacovig, G. Beamson, A. Fondacaro, G. Monaco, G. Vanko, R.G. Egdell, J. Electron. Spectrosc. Relat. Phenom. 169 (2009) 26.
[28] J.H. Scofield, Lawrence Livermore National Laboratory Report UCRL-51326, , 1973.
[29] M.B. Trzhaskovskaya, V.K. Nikulin, V.I. Nefedov, V.G. Yarzhemsky, At. Data Nucl. Data Tables 92 (2006) 245.
[30] A. Walsh, Juarez L.F. Da Silva, Wei Su-Huai, C. Korber, A. Klein, L.F.J. Piper, A. DeMasi, K.E. Smith, G. Panaccione, P. Torelli, D.J. Payne, A. Bourlange, R.G. Egdell, Phys. Rev. Lett. 100 (2008) 167402.
[31] C. Körber, V. Krishnakumar, A. Klein, G. Panaccione, P. Torelli, A. Walsh, J.L.F. Da Silva, S.-H. Wei, R.G. Egdell, D.J. Payne, Phys. Rev. B 81 (2010) 165207.
[32] K.H.L. Zhang, D.J. Payne, R.G. Palgrave, V.K. Lazarov, W. Chen, A.T.S. Wee, C.F. McConville, P.D.C. King, T.D. Veal, G. Panaccione, P. Lacovig, R.G. Egdell, Chem. Mater. 21 (2009) 4353.
[33] D.C. King, T.D. Veal, D.J. Payne, A. Bourlange, R.G. Egdell, C.F. McConville, Phys. Rev. Lett. 101 (2008) 116808.
[34] B. Li, A. Yutaka, J. Li, H. Okushi, I. Sakaguchi, S. Ueda, H. Yoshikawa, Y. Yamashita, S. Senju, K. Kobayashi, M. Sumiya, H. Haneda, N. Ohashia, Appl. Phys. Lett. 98 (2011) 082101.
[35] K. Nomura, T. Kamiya, H. Yanagi, E. Ikenaga, K. Yang, K. Kobayashi, M. Hirano, H. Hosono, Appl. Phys. Lett. 92 (2008) 202117.
[36] K. Nomura, T. Kamiya, E. Ikenaga, H. Yanagi, K. Kobayashi, H. Hosono, J. Appl. Phys. 109 (2011) 073726.
[37] J.J. Kim, E. Ikenaga, M. Kobata, A. Takeuchi, M. Awaji, H. Makino, P.P. Chen, A. Yamamoto, T. Matsuokac, D. Miwa, Y. Nishino, T. Yamamoto, T. Yao, K. Kobayashi, Appl. Surf. Sci. 252 (2006) 5602.
[38] Y. Yamashita, K. Ohmori, S. Ueda, H. Yoshikawa, T. Chikyow, K. Kobayashi, e-J. Surf. Sci. Nanotechnol. 8 (2010) 81.
[39] T. Nagata, M. Haemori, Y. Yamashita, H. Yoshikawa, Y. Iwashita, K. Kobayashi, T. Chikyow, Appl. Phys. Lett. 97 (2010) 082902.
[40] M. Kobata, I. Piš, H. Iwai, H. Yamazui, H. Takahashi, M. Szuki, H.I. Matsuda, H. Daimon, K. Kobayashi, Anal. Sci. 26 (2010) 1.
[41] H. Matsuda, H. Daimon, M. Kato, M. Kudo, Phy. Rev. E 71 (2005) 066503.
[42] I. Pis, M. Kobata, T. Matsushita, H. Nohira, K. Kobayashi, Appl. Phys. Express 3 (2010) 056701.
[43] M. Kobata, I. Pis, H. Nohira, H. Iwai, K. Kobayashi, Surf. Interface Anal. 43 (2011) 1632.